Journal of the Physical Society of Japan
Vol. 76, No. 9, September, 2007, 094713

Dilute Magnetic Semiconductors Based on Half-Heusler Alloys

Tetsuya FUKUSHIMA*, Kazunori SATO,
Hiroshi KATAYAMA-YOSHIDA, and Peter H. DEDERICHS[1]

The Institute of Scientific and Industrial Research (ISIR), Osaka University, 8-1 Mihogaoka, Ibaraki, Osaka 567-0047
[1]*Institut für Festkörperforschung, Forschungszentrum Jülich, D-52425 Jülich, Germany*

(Received June 16, 2007; accepted July 11, 2007; published September 10, 2007)

We have investigated the electronic structure and magnetism of Mn-doped half-Heusler alloys by using the Korringa–Kohn–Rostoker coherent potential approximation (KKR-CPA) method within the local density approximation (LDA). Half-Heusler compounds can be attractive for spintronic applications because the crystal structure and lattice constant of these compounds are similar to those of III–V and II–VI compounds, which are often used in present semiconductor technologies. The Curie temperatures of Mn-doped half-Heusler alloys are calculated by the mean field approximation, random phase approximation, and Monte Carlo simulation. Based on our calculation results, we discuss whether or not the half-Heusler-based dilute magnetic semiconductors are useful for realizing semiconductor spintronics.

KEYWORDS: dilute magnetic semiconductor, half-metallic ferromagnetism, half-Heusler alloy, Curie temperature, double exchange interaction, superexchange interaction, Monte Carlo simulation, exchange coupling constant
DOI: 10.1143/JPSJ.76.094713

1. Introduction

Spintronics has attracted considerable attention in the scientific and industrial fields, because the combination of the two degrees of freedom of the electron spin and the electron charge promises new functionalities. Half-metallic ferromagnetism is essential for realizing spintronic applications.[1,2] In such half-metallic systems, the two spin bands show very different behavior. The majority spin band shows typical metallic behavior with a finite density of states at the Fermi level (E_F), whereas the minority spin band exhibits semiconductor behavior with a band gap at E_F. After half-metallic ferromagnetism was theoretically predicted in a NiMnSb system,[3] researchers have successfully searched for new half-metallic systems such as $La_{1-x}Sr_xMnO_3$, Co_2MnGe, Co_2MnSi, and CrAs.[4–6] These materials might prove useful for applications in metal spintronics, for example, in MRAMs, spin-FETs, magnetic-heads, etc.

Dilute magnetic semiconductors (DMSs) are expected to be one of the materials to realize applications for semiconductor spintronics. Ever since half-metallic ferromagnetism was observed in DMSs,[7] researchers have tried to establish semiconductor spintronics based on DMS materials. The basic challenge is the fabrication of a DMS with a high Curie temperature (T_C), and this has been the subject of many investigations. To obtain a high-T_C in DMSs, magnetic impurity doped III–V and II–VI semiconductors [(Ga,Mn)As, (In,Mn)As, and (Zn,Cr)Te] were mainly examined in the previous efforts.[7–10] In this paper, we focus on semiconducting half-Heusler compounds *XYZ* as host crystals, which are doped with transition metals by replacing Y atoms by Mn atoms. Many interesting physical phenomena such as half-metallic ferromagnetism, thermoelectric conversion, and shape-memory alloys have been discovered with the Heusler alloys.[11] Half-Heusler compounds consist of two transition metal elements *X* and *Y* and one *s*, *p* element *Z*. These compounds with half-metallic ferromagnetism obey a sum rule for the total magnetic moment per unit cell, $M_{total} = Z_{total} - 18$,[12,13] where Z_{total} is the total number of valence electrons in the half-Heusler compounds. According to this rule, half-Heusler compounds with 18 valence electrons (FeVSb, CoTiSb, NiTiSn, NiZrSn, etc.) are expected to be semiconductors. Such half-Heusler compounds can be attractive for spintronic applications since their crystal structure and lattice constant are similar to those of III–V and II–VI compounds, which are often used in present semiconductor technology. In the half-Heusler systems, we can expect strong magnetic interaction between the doped Mn atoms. For instance, in FeVSb, the valence and conduction bands are formed by the *d* states of Fe and V, respectively. Therefore, due to strong d_{Mn}–d_{Fe} hybridisation, the magnetic interaction between Mn atoms is very strong. In addition, for these metallic systems, the solubility should be much higher since many ordered compounds exist and no major problems with compensation defects are expected. Tobola *et al.*,[14] and Nanda and Dasgupta[15] have already investigated the electronic structures of Mn-doped half-Heusler semiconductors by first-principles calculations. However, accurate investigations of the exchange coupling constants and T_C were not included in their studies. The main purpose of this study is to calculate the exchange coupling constants and T_C of Mn-doped half-Heusler compounds by using first-principles calculations and the Monte Carlo method. Based on our calculated results, we discuss whether a half-Heusler type DMS is effective for the realization of spintronic applications.

Our calculational method is briefly summarized in §2. The results are presented and discussed in §3. Section 4 is devote to the summary of our study.

2. Calculational Method

Our calculational procedure is divided into three parts. First, the electronic structure and magnetism of Mn-doped half-Heusler compounds are calculated by the Korringa–

*E-mail: fuku@cmp.sanken.osaka-u.ac.jp

Kohn–Rostoker method combined with coherent potential approximation (KKR-CPA) within the local density approximation (LDA) of density functional theory.[16,17] The CPA is the most accurate single site method for a disordered system, and the KKR-CPA is the most sophisticated implementation to treat the electronic structure of disordered compounds. To take the relativistic effects into account, the scalar relativistic approximation is employed. The form of the potential is restricted to the muffin-tin type. The unit cell of a half-Heusler structure ($C1_b$ structure) XYZ consists of three fcc sublattices with basis atoms X at $(0,0,0)$, Y at $(1/4,1/4,1/4)$, and Z at $(3/4,3/4,3/4)$. In the Mn-doped half-Heusler type DMS, the Y sites are randomly substituted with Mn atoms. One extra empty muffin-tin potential at $(1/2,1/2,1/2)$ is used in addition to those of the normal atomic sites in our calculation. Lattice distortions due to impurity doping are neglected and experimental lattice constants of semiconducting half-Heusler compounds are used.[18]

Next, in order to estimate the strength of the magnetic interaction between Mn atoms, we calculate the exchange coupling constants J_{ij} between two Mn atoms at sites i and j as a function of distance. The method developed by Liechtenstein *et al.* is used for the calculation.[19] According to this method, two Mn atoms are embedded into the ferromagnetic CPA medium generated by the KKR-CPA method and then the exchange coupling constants are calculated by mapping the total energy change due to infinitesimal rotations of the two Mn moments at sites i and j to the classical Heisenberg model. As a result, J_{ij} is given by

$$J_{ij} = \frac{1}{4\pi} \mathrm{Im} \int^{E_F} \mathrm{d}E \, \mathrm{Tr}_L \{\Delta_i T_{\uparrow}^{ij} \Delta_j T_{\downarrow}^{ji}\}, \tag{1}$$

where $\Delta_i = t_{i\uparrow}^{-1} - t_{i\downarrow}^{-1}$, $t_{i\uparrow(\downarrow)}^{-1}$ is the atomic t-matrix of the magnetic impurities at site i for the spin up (down) state. $T_{\uparrow(\downarrow)}^{ij}$ is the scattering path operator between sites i and j for the spin up (down) state. Tr_L is the trace over the orbital variables.

Finally, based on the results of first principles calculations, the T_Cs of Mn-doped half-Heusler compounds are calculated by using the mean field approximation (MFA), the random phase approximation (RPA), and the Monte Carlo simulation (MCS). Within the MFA, we can calculate T_C^{MFA} from

$$k_B T_C^{\mathrm{MFA}} = \frac{2}{3} c \sum_{n \neq 0} J_{n0}, \tag{2}$$

where c is the Mn concentration and k_B is the Boltzmann constant. As pointed out by Sato[20] and Bergqvist,[21] the MFA strongly overestimates the T_C due to the lack of describing the magnetic percolation effect. On the other hand, the RPA and MCS take the magnetic percolation effect into consideration and predict the T_C accurately; in particular, the MCS gives the exact numerical value. In the RPA, T_C^{RPA} is calculated by using the Tyablikov decoupling for magnon Green's function.[22,23] According to this method, we can calculate the T_C^{RPA} by

$$k_B T_C^{\mathrm{RPA}} = \frac{2}{3} \left(\frac{1}{N} \sum_r \frac{1}{E_r} \right)^{-1}, \tag{3}$$

where N is the number of Mn atoms and E_r is the eigenvalue of the Hamiltonian matrix H, which is defined by $H_{ij} = \delta_{ij}(\sum_{n=1}^{N} J_{in}) - J_{ij}$. For the MCS, we use the 4th order cumulant intersection method by Binder, which is based on finite size scaling.[24] The 4th order cumulant for magnetization is calculated by

$$U_L(T) = 1 - \frac{\langle M^4 \rangle}{3\langle M^2 \rangle^2}. \tag{4}$$

T_C^{MCS} is calculated from the intersection of the 4th order cumulant for three super cell sizes ($10 \times 10 \times 10$, $14 \times 14 \times 14$ and $18 \times 18 \times 18$). In the MCS, T_C can be accurately calculated within the statistical error and the classical Heisenberg model. Exchange coupling constants up to 15 shells are included in this simulation. We take 30 different random configurations of magnetic sites for the ensemble average and perform 240000 Monte Carlo steps.

3. Results of the Calculations

Figure 1 shows the density of states of Mn 10% doped (a) FeVSb, (b) CoTiSb, (c) NiTiSn, and (d) NiZrSn calculated by the KKR-CPA method. As pointed out above, these hosts are half-Heusler semiconductors with $Z_{\mathrm{total}} = 18$. As in the zinc-blende type DMS, the Mn atoms are tetrahedrally coordinated, so the behavior in the band gap is dominated by the Mn e_g and t_{2g} states. The e_g states lie energetically below the t_{2g} states, which hybridize strongly with the valence d states of Fe, Co, or Ni atoms. Thus, the behavior is similar to that of Mn in compound semiconductors like (Ga,Mn)As, where the Mn t_{2g} states hybridize strongly with the p states of the As valence band. In the Mn-doped FeVSb system, as shown in Fig. 1(a), by replacing V with Mn atoms two electrons of Mn fill the e_g state, and the t_{2g} states are completely empty. The total magnetic moment, located mostly at the Mn atom, can be easily estimated to be $2\mu_B$ for Fe(V,Mn)Sb. As a result, the Fermi level is located between the e_g and the t_{2g} states. In this case, it is suggested that the superexchange interaction becomes ferromagnetic for the combination of the Mn-d states in the tetrahedral symmetry.[25–27] The electronic structure of Fe(V,Mn)Sb is very similar to those of V-doped III–V systems.[28] On the other hand, the other systems show a different behavior of density of states. As shown in Figs. 1(b)–1(d), one more electron fills one of the three Mn t_{2g} states and the Fermi level lies within the Mn t_{2g} impurity band. Therefore, similar to the (Ga,Cr)N system, the total magnetic moment per Mn atom of Co(Ti,Mn)Sb, Ni(Ti,Mn)Sn, and Ni(Zr,Mn)Sn can be estimated to be $3\mu_B$. In this situation, due to the broadening of the Mn t_{2g} impurity band with an increasing Mn concentration, the state weight is transferred to a lower energy, leading to energy gain and stabilization of ferromagnetism.[28,29] This ferromagnetic interaction is called Zener's double-exchange interaction. The positions of the t_{2g} states are similar to those of (Ga,Mn)As, which stabilizes the ferromagnetism by the p–d exchange interaction; however, the double-exchange interaction in this case dominates since the t_{2g} states are occupied by one electron only and are somewhat higher in energy.

Figure 2 shows the exchange coupling constants J_{ij} of Fe(V,Mn)Sb, Co(Ti,Mn)Sb, Ni(Ti,Mn)Sn, and Ni(Zr,Mn)Sn calculated by Liechtenstein's formula as a function of

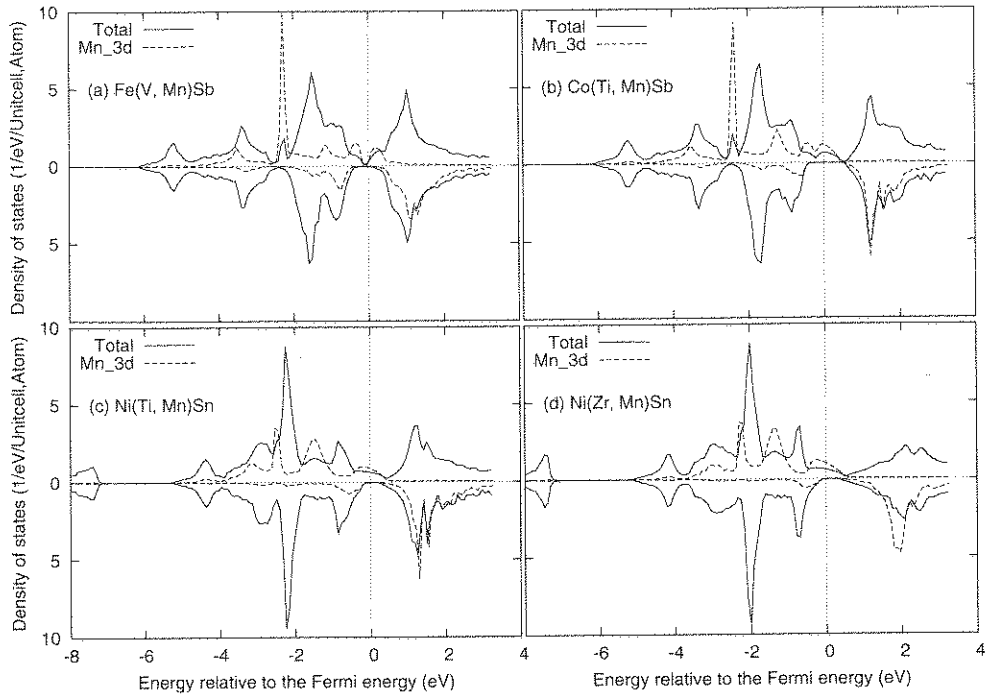

Fig. 1. Calculated density of states of Mn 10% doped (a) FeVSb, (b) CoTiSb, (c) NiTiSn, and (d) NiZrSn by using the KKR-CPA method. The solid and dashed lines indicate total and partial Mn d density of states, respectively. The horizontal axis shows the energy relative to the Fermi level. The lower table shows the local and total magnetic moments of the Mn atoms in Mn 10% doped half-Heusler alloys (in μ_B).

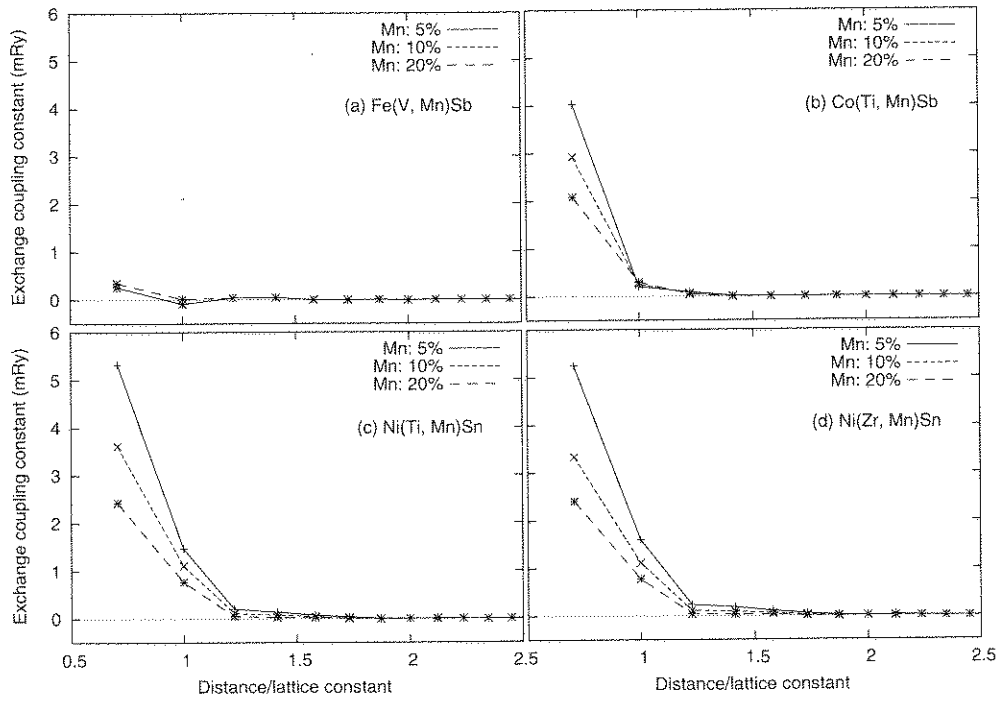

Fig. 2. Calculated exchange coupling constants of Mn doped (a) FeVSb, (b) CoTiSb, (c) NiTiSn, and (d) NiZrSn as a function of the distance between two Mn atoms by using Liechtenstein's formula. Mn 5% (solid lines), 10% (dotted lines), and 20% (dashed lines) cases are indicated, respectively.

the distance between two Mn atoms. Mn 5, 10, and 20% cases are shown in the figure. In the case of Fe(V,Mn)Sb, the exchange coupling interactions are very small and do not depend on the Mn concentration. This behavior is a typical case for ferromagnetic DMS stabilized by the superexchange interaction. On the other hand, as shown in Figs. 2(b)–2(d), the exchange coupling constants of Co(Ti,Mn)Sb, Ni(Ti,Mn)Sn, and Ni(Zr,Mn)Sn are strong only for the nearest neighbors and decay exponentially with the distance between two Mn atoms. This is because the wave function for deep impurity states in the band gap decays exponentially. Such short-ranged interactions affect many physical quantities such as Curie temperature, electric conductivity, magnon dispersion, etc., in the dilute

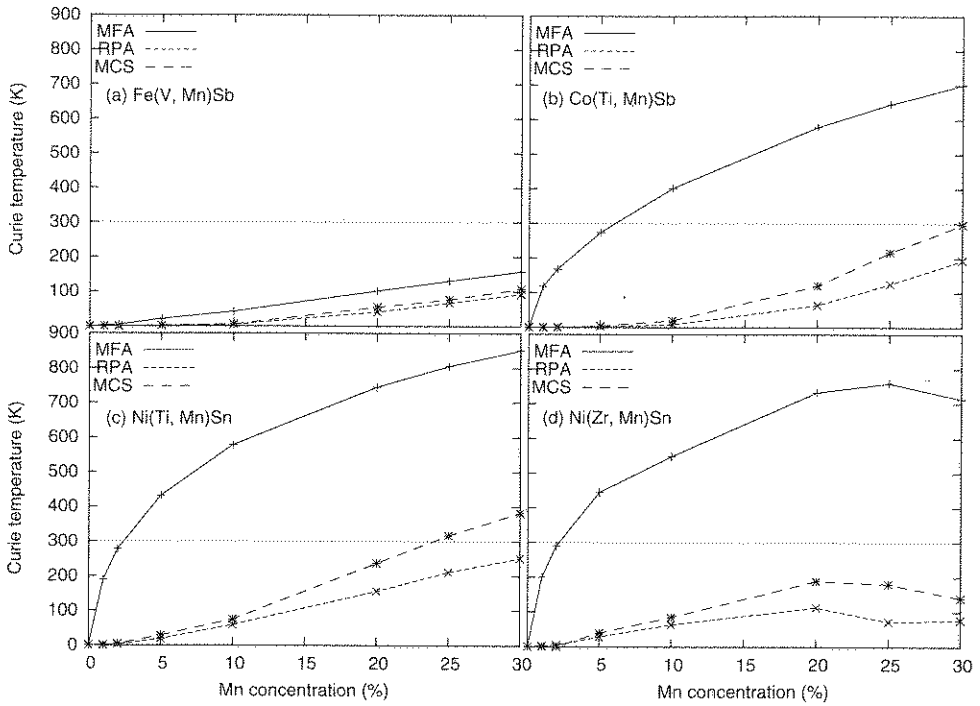

Fig. 3. Calculated Curie temperatures of Mn-doped (a) FeVSb, (b) CoTiSb, (c) NiTiSn, and (d) NiZrSn as a function of the Mn concentration. The Curie temperature is calculated by mean field approximation (MFA; solid lines), random phase approximation (RPA; dotted lines), and Monte Carlo simulation (MCS; dashed lines).

systems. The values of the nearest neighbor's coupling for Co(Ti,Mn)Sb, Ni(Ti,Mn)Sn, and Ni(Zr,Mn)Sn are stronger than those of (Ga,Mn)As[20,21] and even of (Zn,Cr)Te.[30] Therefore, we can expect high-T_C values for Mn-doped Co(Ti,Mn)Sb, Ni(Ti,Mn)Sn, and Ni(Zr,Mn)Sn in the high concentration region.

Figure 3 shows the T_Cs of (a) Fe(V,Mn)Sb, (b) Co(Ti,Mn)Sb, (c) Ni(Ti,Mn)Sn, and (d) Ni(Zr,Mn)Sn calculated by using MFA, RPA, and MCS. The horizontal axis denotes the Mn concentration. For estimating the T_C of DMS, the magnetic percolation effect is very important because below the percolation threshold, the ferromagnetic interaction cannot spread over the entire crystal.[20,21] If only the nearest neighbor's interaction is considered, the percolation threshold is 20% for the fcc lattice. The MFA overestimates the T_C since it cannot take the magnetic percolation effect into account. As understood from the MFA equation, the dilution effect is included only as a concentration factor c. In Fe(V,Mn)Sb, ferromagnetic superexchange interaction is very weak and shows a linear c dependence for the T_C^{MFA} since the energy gain by ferromagnetic superexchange interaction is given by $c(t^2/\Delta E_{CF})$, where t is the effective hopping matrix element between the e_g and the t_{2g} states, and ΔE_{CF} is the crystal filed splitting. In the other systems, as shown in Figs. 3(b)–3(d), the T_C^{MFA} is approximately proportional to $\sqrt{c}$. We can understand this concentration dependence by considering the double exchange mechanism. The energy gain in the ferromagnetic state is proportional to the band width in the double exchange mechanism. This explains the $\sqrt{c}$ behaviors, since the band width of the impurity bands is proportional to $\sqrt{c}$ according to the CPA theory. In Ni(Zr,Mn)Sn, the T_C^{MFA} value saturates at approximately Mn 25%, then decreases with the Mn concentration. This strong suppression of ferromagnetism for high concentrations is due to an anti-ferromagnetic contribution of the superexchange interaction. On the other hand, RPA and MCS, which take the magnetic percolation effect into account, provide a more realistic estimation of the T_C. As shown in Fig. 3, below the percolation threshold, all systems show the paramagnetic state or ferromagnetic state with a very low T_C value. We can understand the paramagnetic or weakly ferromagnetic behavior from the fact that for low concentrations, the nearest neighbor's interaction can only make small non-interacting clusters in which the interaction aligns the magnetic moments in the small clusters well, but cannot spread over the entire crystal. When the Mn concentration increases and reaches the percolation threshold, the strong nearest neighbor's interaction can percolate the entire crystal. As a result, in the high Mn concentration region, room temperature ferromagnetism can be expected because the main contribution to ferromagnetism, as shown in Fig. 2, is the nearest neighbor's interaction. However, in the low concentration region below 10%, the calculated T_Cs are very low, which is similar to the results for compound semiconductors.[20,21]

4. Summary

In order to fabricate DMS based on half-Heusler alloys, we have investigated the electronic structures and magnetism of Mn-doped half-Heusler semiconductors (FeVSb, CoTiSb, NiTiSn, and NiZrSn) by using first principles calculations. From the magnetic behavior point of view, these systems are very similar to transition metal doped III–V and II–VI compounds.[28,30] The electronic structures of these systems are determined by the localized e_g states and the strongly hybridising t_{2g} states in the band gap. For Mn-doped FeVSb, the Fermi level is located between the e_g

and the t_{2g} states, and the ferromagnetic state is stabilized by the ferromagnetic superexchange interaction. In the other systems, the e_g states are fully occupied and the threefold degenerate t_{2g} states are occupied by one electron only. As a result, the double exchange interaction stabilizes ferromagnetism in these systems. The Curie temperatures of Mn-doped half-Heusler alloys have been calculated by mean field approximation, random phase approximation, and Monte Carlo simulation. As for the compound semiconductor systems, mean field approximation strongly overestimates the Curie temperature. According to our results, Mn-doped CoTiSb and NiTiSn have room temperature ferromagnetism for high Mn concentration of approximately 25–30%. If the high concentration doping is possible, realization of the semiconductor spintronics can be expected by using half-Heusler type dilute magnetic semiconductors. However, since many ordered half-metallic Heusler alloys like NiMnSb or CoMnSb exist and have high Curie temperatures, it is not clear if these disordered Heusler alloys will have advantages for spintronics applications.

Acknowledgment

This research was partially supported by a Grant-in-Aid for Scientific Research in Priority Areas "Quantum Simulators and Quantum Design" (No. 17064014), a Grant-in-Aid for Scientific Research for young researchers, JST-CREST, NEDO-nanotech, the 21st Century COE and the JSPS core-to-core program "Computational Nano-materials Design". This research was also supported in part by the National Science Foundation under Grant No. PHY99-07949, the Kansai Research Foundation (KRF) for technology promotion, Foundation for c & c Promotion, the Murata Science Foundation, and the Inoue Foundation for Science (IFS).

1) H. Ohno: Science **281** (1998) 951.
2) H. Ohno: Science **291** (2001) 840.
3) R. A. de Groot, F. M. Mueller, P. G. van Engen, and K. H. J. Buschow: Phys. Rev. Lett. **50** (1983) 2024.
4) W. Pickett and D. Singh: Phys. Rev. B **53** (1996) 1146.
5) S. Ishida, S. Fujii, S. Kashiwagi, and S. Asano: J. Phys. Soc. Jpn. **64** (1995) 2152.
6) H. Akinaga, T. Manago, and M. Shirai: Jpn. J. Appl. Phys. **39** (2000) L1118.
7) H. Munekata, H. Ohno, S. von Molnar, A. Segmüller, L. L. Chang, and L. Esaki: Phys. Rev. Lett. **63** (1989) 1849.
8) F. Matsukura, H. Ohno, A. Shen, and Y. Sugawara: Phys. Rev. B **57** (1998) R2037.
9) H. Saito, V. Zayets, S. Yamagata, and K. Ando: Phys. Rev. Lett. **90** (2003) 207202.
10) N. Ozaki, N. Nishizawa, S. Marcet, S. Kuroda, O. Eryu, and K. Takita: Phys. Rev. Lett. **97** (2006) 037201.
11) Materia Japan **44** (2005) No. 8 [in Japanese].
12) I. Galanakis and P. H. Dederichs: *Half-Metallic Alloys* (Springer, Berlin, 2005) p. 12.
13) I. Galanakis, P. Mavropoulos, and P. H. Dederichs: J. Phys. D **39** (2006) 765.
14) J. Tobola, S. Kaprzyk, and P. Pecheur: Phys. Status Solidi B **236** (2003) 531.
15) B. R. K. Nanda and I. Dasgupta: J. Phys.: Condens. Matter **17** (2005) 5037.
16) H. Akai and P. H. Dederichs: Phys. Rev. B **47** (1993) 8739.
17) H. Akai: http://sham.phys.sci.osaka-u.ac.jp/~kkr/
18) P. J. Webster and K. R. A. Ziebeck: *Alloys and Compounds of d-Elements with Main Group Elements* (Springer, Berlin, 1988) p. 75.
19) A. I. Liechtenstein, M. I. Katsnelson, V. P. Antropov, and V. A. Gubanov: J. Magn. Magn. Mater. **67** (1987) 65.
20) K. Sato, W. Schweika, P. H. Dederichs, and H. Katayama-Yoshida: Phys. Rev. B **70** (2004) 201202.
21) L. Bergqvist, O. Eriksson, J. Kudrnovský, V. Drchal, P. Korzhavyi, and I. Turek: Phys. Rev. Lett. **93** (2004) 137202.
22) G. Bouzerar, T. Ziman, and J. Kudrnovský: Europhys. Lett. **69** (2005) 812.
23) S. Hilbert and W. Nolting: Phys. Rev. B **70** (2004) 165203.
24) K. Binder and D. W. Heermann: *Monte Carlo Simulation in Statistical Physics* (Springer, Berlin, 2002) p. 39.
25) J. Kanamori: J. Phys. Chem. Solids **10** (1959) 87.
26) J. B. Goodenough: Phys. Rev. **100** (1955) 564.
27) H. Katayama-Yoshida, K. Sato, T. Fukushima, M. Toyoda, H. Kizaki, V. A. Dinh, and P. H. Dederichs: J. Magn. Magn. Mater. **310** (2007) 2070.
28) K. Sato, H. Katayama-Yoshida, and P. H. Dederichs: Semicond. Sci. Technol. **17** (2002) 367.
29) H. Akai: Phys. Rev. Lett. **81** (1998) 3002.
30) T. Fukushima, K. Sato, H. Katayama-Yoshida, and P. H. Dederichs: Jpn. J. Appl. Phys. **43** (2004) L1416.